FIRE PROTECTION & SAFETY Scientific Journal
16(1): 17–37, 2022
DOI: 10.17423/delta.2022.16.1.105

Experimental Investigation of Digital Image Analysis Opportunities for Studying the Wildfire Dynamics

Radovan Hilbert [1,*], Ivan Kubovský [2], Andrea Majlingová [3]

[1] Technical university in Zvolen, Faculty of Wood Sciences and Technology, Department of Fire Protection, T.G. Masaryka 24, 960 01 Zvolen, Slovakia; xhilbert@is.tuzvo.sk

[2] Technical university in Zvolen, Faculty of Wood Sciences and Technology, Department of Physics, Electrical Engineering and Applied Mechanics, T.G. Masaryka 24, 960 01 Zvolen, Slovakia; kubovsky@tuzvo.sk

[3] Technical university in Zvolen, Faculty of Wood Sciences and Technology, Department of Fire Protection, T.G. Masaryka 24, 960 01 Zvolen, Slovakia; majlingova@tuzvo.sk

[*] Corresponding author: majlingova@tuzvo.sk

Original scientific paper

Received: 15.07.2022; Accepted: 27.07.2022; Published: 31.07.2022

Abstract

The ongoing climate change and observed impacts on the wildland puts in the foreground the need to study the behaviour of wildfires also in the conditions of Central Europe. This study deals with an investigation of beech forest litter fire behaviour. The main objective of study was the identification and verification of opportunities of digital image analysis application in fire engineering and development of a methodology for automated image processing and derivation of selected parameters necessary for describing fire dynamics from images produced by thermal imaging (infrared band) and optical cameras. There were totally five fire tests provided, while three of them were carried out in a laboratory chamber with the simultaneous use of an optical (video) camera used to record the development of flame burning in time. The other two fire tests were carried out in a laboratory fume hood with simultaneous recording of the fire propagation with the Fluke RSE600 thermal imaging camera from above and with an optical camera from the front. For images pre-processing and processing several software were used. Methodologies were developed to derive selected parameters of fire dynamics, which enable wider and more complex use of knowledge obtained from records from a thermal imaging camera, as well as from classic video camera. The results of the study have their application in science and in practice. From the point of view of application in science, they point to the possibilities and suitability of the application in the work of applied digital technologies for the study of fire behaviour and the automated derivation of its selected parameters. The study provides guidance for conducting similar experiments using digital technologies aimed at studying fire behaviour, too.

Keywords: digital image analysis; fire dynamics, forest litter, wildfire fire

1 Introduction

Protecting the population from the effects of emergencies is one of the key tasks of civil protection in Slovakia. Among such emergencies, specifically natural disasters, belongs also wildfire.

Uncontrollably spreading fires of forest vegetation, grasslands and agricultural crops are a global phenomenon [1,2] that can be linked by expected climatic and meteorological conditions. They often lead to large-scale disasters that result in significant adverse economic, social, and environmental consequences [3-5].

Fire is a complex phenomenon involving many processes (for example, the process of burning, release, and transfer of energy) that occur over a wide range of spatial and temporal scales. The characteristics of the fuel particles and the structure of the fuel itself partly determine the amount of energy that will be released in the process of its combustion and describe the way in which the process of combustion and heat transfer takes place [1,6]. Knowledge of the relevant characteristics of fuel occurring in the wildland, which influence fire behaviour, is essential for informing and supporting the decision-making process of relevant persons, as well as input for a wide range of applications intended for fire management (control) as well as the planning of preventive measures aimed at mitigating the occurrence of large fires [7,8]. These applications can be aimed at assessment of the fire danger and providing fire warnings [9-11], assessing the wildfire risks [12,13], modelling the behaviour of fires occurring in different types of vegetation (e.g. grasslands, forests, bushes), planning tactical procedures for fire elimination, calculation of emissions of combustion products arising during a fire [1] and predicting the effects of a fire from the point of view of several aspects [14,15].

Currently, it is often discussed in professional circles as well as among the lay public that the main cause of the increased frequency of fires in wildland is the ongoing climate change and especially its impacts. However, the latest findings of experts [3] show that the danger of wildfires will increase despite the effects of climate change. Several factors contribute to their increased occurrence, such as the moisture content of fine fuel that occurs on the surface of the ground, but also material of larger dimensions, such as pieces of wood. Sufficiently wet surface of the material can reduce the potential of fire spread and positively influence its flammability. Meteorological factors such as wind speed are also important as they can affect the speed at which a fire could spread once it is ignited. [4] However, a critical factor related mainly to extreme weather (periods of prolonged drought) is the moisture content of coarse woody fuels and other organic matter on the ground. And this will be the most significant problem, especially during periods of long drought.

From the above, it is obvious that there is a need to solve the problem of wildfires and in general to research the dynamics of wildfires even in the conditions of Central Europe, where until now they have not been among the significant and frequently occurring natural disasters. The study presented here, and its results, are a contribution to the solution of this issue precisely at the level of the Central European region, which is characterized by the similarity of its geographical, vegetational and climatic conditions.

The main objective of the study was to identify and verify the suitability of applications of digital image analysis tools in fire engineering, i.e., automated image processing and derivation of selected parameters necessary for describing forest fire behaviour from infrared images recorded by a Fluke RSE600 thermal imaging camera and video (optical) camera during laboratory experiments with beech forest litter in a dry state.

Images obtained from video cameras and infrared (thermal imaging) cameras have been used, especially abroad, for several years to study the spread of forest fire fronts, to determine the height of the flame during a fire, the depth of fuel and the angle of inclination of the flame burning along the fire front [16-19] and even to measure the velocity field in the convection column above the fire front [20,21] and the intensity of radiant heat and flame temperature fields [22]. An experimental method using digital image processing techniques obtained from a combination of optical (video) and infrared cameras was already presented by Martínez-de-Dios et al. [23,24]. The images captured the spreading front of the fire, taken from one or more cameras to obtain the time course of the shape and position of the fire front, the angle of inclination of the flame, the height and width of the fuel base.

2 Material and Methods

The material that was investigated was the forest litter collected in the beech forest (stand no. 551, located on the territory of the University Forestry Enterprise of the Technical University in Zvolen) on August 17, 2021. This stand was characterized by the following woody vegetation: European beech 95%, Silver fir 2%, European larch 2% and Sessile oak 1%. The age of the stand was of 60 years.

The sampled beech litter was dried to a dry state in the MEMMERT air dryer before the fire tests were carried out, and in this state, it was also used in individual experiments, in the amount of 100 g for

each test. The duration of each experiment was set to 10 min. While the following data were also recorded during the test: end of flame burning, end of glowing and smouldering.

Laboratory fire tests (5 tests totally) were carried out using the available research infrastructure of the Combustion Laboratory, which is managed by the Department of Fire Protection. The fire tests were carried out in two phases. In the first phase, three fire tests were carried out in the laboratory chamber, together with providing video recordings of the flames.

In the second phase, two fire tests were carried out using not only a video camera, but also a thermal imaging camera. These were carried out in the MERCI G laboratory hood. Here we consider it necessary to emphasize that the implementation of the fire tests served exclusively the purpose of obtaining a basic set of data, i.e., images that were the basis for the processing of image analyses and the development of methodologies for automated image processing and the derivation of selected parameters of fire dynamics.

The experiments were performed using a circular test dish with a diameter of 50 cm and a height of 3 cm. During the experiments, the mass loss of the fuel was recorded at intervals of 10 s. RADWAG WLC R2 precision scales were used for this purpose. Thermocouples (T1 – T5) connected to an autonomous measuring station ALMEMO®710 by AHLBORN and a Fluke RSE600 thermal imaging camera providing a sequence of images with a temporal resolution of 8.6 frames per 1 s and a spatial resolution of 640 x 480 pixels were used to record the course of temperatures during the fire.

The GoPro4 video camera was used to create videos of the fire tests. These records were used in a later phase to derive selected flame parameters applying digital image analysis tools.

From the provided laboratory fire tests, data on the course of temperatures recorded by individual thermocouples (T1-T5) were obtained and further analysed.

Using the RADWAG precision scales, the mass loss of the samples was recorded during the 10-min lasting fire tests. These were processed into graphs. From these data, we also calculated the relative mass loss (1) and the relative mass burning rate (2) in time:

$$\delta_m(\tau) = \frac{\mathrm{m}(\tau_0) - \mathrm{m}(\tau)}{\mathrm{m}\,(\tau_0)} \cdot 100 \qquad (\%) \qquad (1)$$

$$v_r = \frac{\delta_m(\tau) - \delta_m\,(\tau + \Delta\tau)}{\Delta\tau} \cdot 100 \qquad (\%\cdot s^{-1}) \qquad (2)$$

Where:

$\delta_m(\tau)$ – relative mass loss in time (%)
v_r – relative rate of burning (%·s^{-1})
$\Delta\tau$ – time interval in which the weights are recorded (s)
$\delta_m(\tau + \Delta\tau)$ – relative mass loss in time (%)

Data on the surface temperature of the fuel at the positions of the thermocouples, which recorded the temperature inside the fuel, were processed from the records obtained by the thermal imaging camera. Subsequently, these temperatures were compared with each other, and the results were analysed and discussed.

The course of temperatures on the surface of the fuel was also recorded and analysed on other profiles, both within the entire surface of the test dish and on specified profiles across the test dish.

From the thermal imaging records, video records and observations, the duration of the flame burning and the time of the glowing (smouldering) of the fuel were obtained. These times were compared to each other. Conclusions were drawn from the results of the comparison.

Data on the mean, average and maximum height of the flame during the fire tests were derived from the data acquired by the video camera. These were derived from images for each 5 s interval.

To calculate the flame height (L_f), it was first necessary to define the mean flame height (m). This is best to determine by averaging the visible height of the flame as a function of time. This is the height at which the flame appears in half of the time (equation 3).

Equation (3) considers the height of continuous (L_{fk}) and pulsating flame (L_{fp}) in half of the flame burning time.

$$L_f = \frac{L_{fk}+L_{fp}}{2} \quad \text{(m)} \tag{3}$$

We calculated the average flame height as the average of all flame heights recorded at 5 s intervals during flame burning.

The maximum flame height we determined based on the highest flame height value from the flame height values recorded at 5 s intervals during the flame burning.

Using the data from the fire tests carried out in laboratory fume hood, we calculated the density of the radiated heat flux (mm) according to the formula (4) for each pixel of the image (Wien's displacement law):

$$\lambda_{max} = \frac{b}{T} \tag{4}$$

Where:

λ_{max} – wavelength at which, at temperature (T), the radiation intensity is maximum
b – universal constant 2.898 (mm·K)
T – thermodynamic temperature on surface of the material (°C)

In the Idrisi TerrSet environment, input images were processed applying image analysis tools (Idrisi Image Processing), i.e., images obtained every 5 s from video recordings and representing the course of fire tests in a specific time. Those further underwent thresholding and reclassification. As a result, we got 2D flame shapes outlines, which were further used for flame heights calculation.

The rate of burning was calculated based on the mass loss of the sample recorded during the experiments at 10 s intervals.

3 Results and Discussion

In this chapter, we present the results of fire tests, the results of image analysis processing aimed at deriving selected parameters of fire dynamics.

3.1 Temperature course in a fire

In this subsection, we present the results of the fire tests namely, temperature curves obtained from data from individual thermocouples (T1 – middle of the bowl, T2 – western edge of the bowl, T3 – northern edge of the bowl, T4 – eastern edge of the bowl, T5 – southern edge of the bowl) located inside the layer of beech litter and also the course of temperatures measured on the surface of the test sample using a Fluke RSE600 thermal imaging camera. The results presented here were obtained during the laboratory fire tests and from processing of the thermal imaging images (in the SmartView R&D software) and of video recordings.

3.1.1 Temperature course – data from the thermocouples

Thermocouples T1-T5 were in the middle of the fuel complex placed on a circular test dish with a height of 3 cm and a diameter of 50 cm. Thermocouple T1 was in the centre of the test dish and the other thermocouples were located 2 cm far from the dish edge.

Fig. 1-3 show the results for the fire tests carried out in the laboratory chamber.

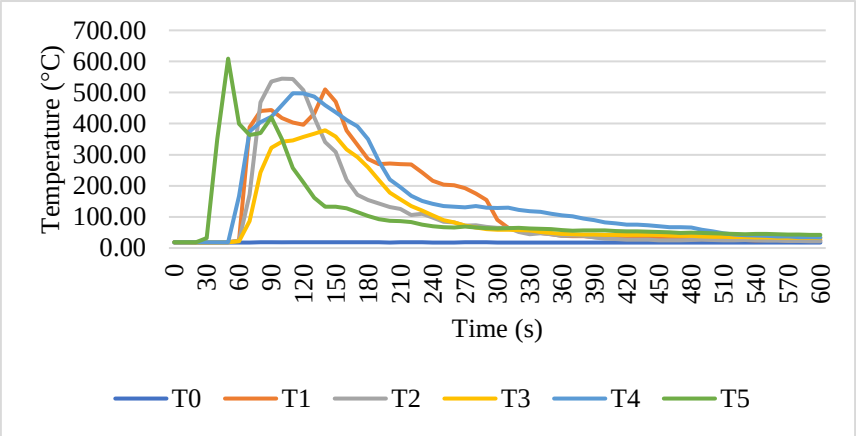

Fig. 1 Temperature course during fire test 1 (chamber) recorded by thermocouples T1-T5

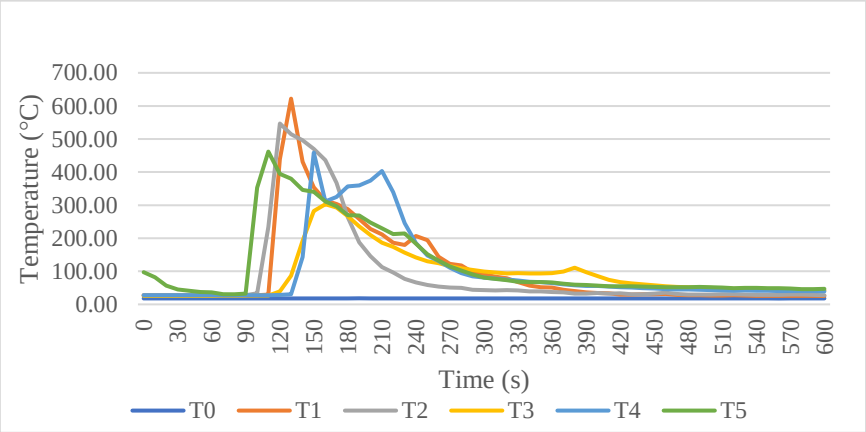

Fig. 2 Temperature course during fire test 2 (chamber) recorded by thermocouples T1-T5

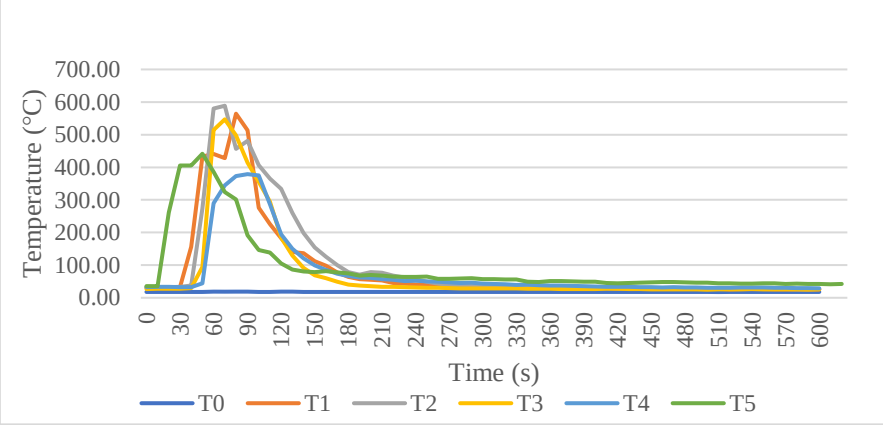

Fig. 3 Temperature course during fire test 2 (chamber) recorded by thermocouples T1-T5

From the course of the provided fire tests, it is obvious that the different course of temperatures in the individual experiments. Combustion was initiated by igniting the fuel in the centre of the test dish (thermocouple T1). Thermocouple T0 recorded the temperature of the surrounding environment. In Tab. 1, we present the maximum temperature values reached on thermocouples T1-T5 during all three tests carried out in the laboratory chamber.

Tab. 1 Maximum temperature values reached by thermocouples – fire tests in the chamber

Fire test /Thermocouple	1		2		3	
	T MAX (°C)	Time (s)	T MAX (°C)	Time (s)	T MAX (°C)	Time (s)
T1 (C)	510.0	140	622.0	130	564.3	80
T2 (W)	549.6	100	546.8	120	588.7	70
T3 (N)	378.7	140	302.7	160	547.0	70
T4 (E)	497.6	110	402.9	210	379.0	90
T5 (S)	420.2	90	461.9	110	441.5	50

*Note: W – west direction; N – north direction; E – east direction; S – south direction; C – centre.

From the results shown in Tab. 1, it is possible to deduce that the heating of the fuel occurred gradually, depending on the direction in which the fire front progressed and where the fire controlled by the available fuel later occurred (maximum temperatures reached during further burning of the fuel). Since the ignition of the fuel always occurred in the centre of the test dish, it is obvious, for example in fire test 1, that the fire front moved from the centre of the test dish first towards the West (T2) and towards the East (T4), i.e., especially in the horizontal direction, slower in the vertical direction. In the case of fire test 2, the front of the fire moved faster especially towards the West (T2) and South (T5). In the case of fire test 3, it spread fastest in the Western (T2) and Northern (T3) directions.

Next, we present the results for the fire tests carried out in the laboratory fume hood (Figures 4 and 5). The obtained results were validated based on knowledge obtained from the study of thermal (infrared) imaging records.

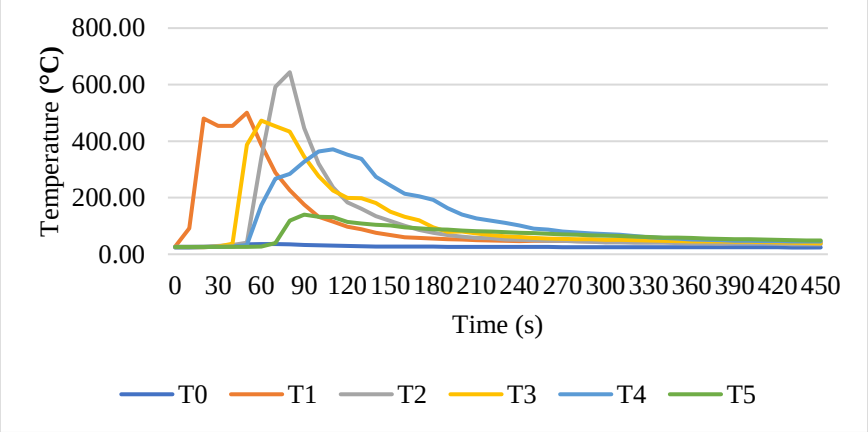

Fig. 4 Temperature course during fire test 1 (fume hood) recorded by thermocouples T1-T5

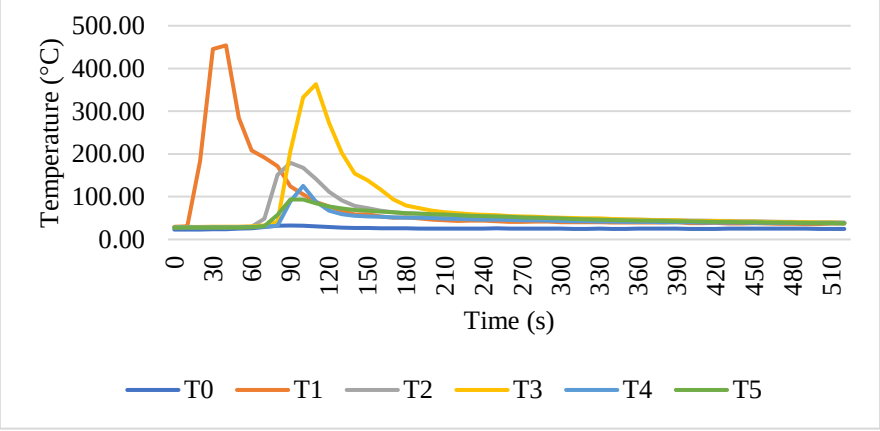

Fig. 5 Temperature course during fire test 2 (fume hood) recorded by thermocouples T1-T5

Like the case of the fire tests carried out in the laboratory chamber, significant differences during both experiments were also seen in the case of the tests carried out in the laboratory fume hood. In Tab. 2 we present the maximum temperature values reached on thermocouples T1-T5 during both tests.

Tab. 2 Maximum temperature values reached by thermocouples – fire tests in the fume hood

Fire test /Thermocouple	1		2	
	T MAX (°C)	Time (s)	T MAX (°C)	Time (s)
T1 (C)	500.7	50	454.1	40
T2 (W)	644.0	80	179.3	90
T3 (N)	472.7	60	363.3	110
T4 (E)	371.1	110	125.3	100
T5 (S)	140.1	90	93.4	90

From the results presented in Table 3, we deduce that due to the above-mentioned principle of evaluating the results, in the case of fire test 1, the fire front moved first towards the Western and Northern edges of the dish. In the case of fire test 2, the fire front moved first towards the Northern (upper) edge.

Images from a thermal imaging camera were used to validate the findings presented here. The results of the analysis of thermal imaging images pointed to the following facts. In fire test 1, the fire front moved fastest to the North, or Northwest, where it reached the Northern edge of the test dish (T3) already in time of 43 s (Fig. 6).

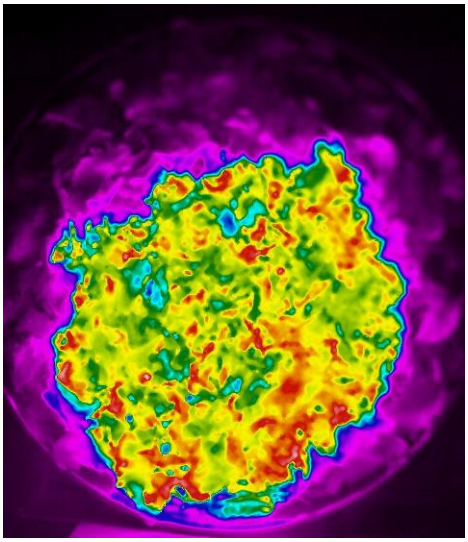

Fig. 6 Fire front reached edge of the test dish – fire test 1

Subsequently, the fire front reached the Western edge of the test dish at 56 s, the Eastern edge at 65 s, and the Southern edge of the dish at 67 s from the start of the fire test. Also, for this reason, considering the amount and structure of available fuel storage, the highest combustion temperatures were later reached at those positions.

In the case of fire test 2, the assumption about the spread of the fire front was not confirmed. Based on the results of the digital image analysis of the infrared images, the fire front moved significantly towards the Northern edge of the test dish at the beginning (Figure 7), but later it spread mainly towards the Southern edge, which reached at time of 61 s. The western edge of the test dish was reached at time of 64 s from the beginning of the fire test.

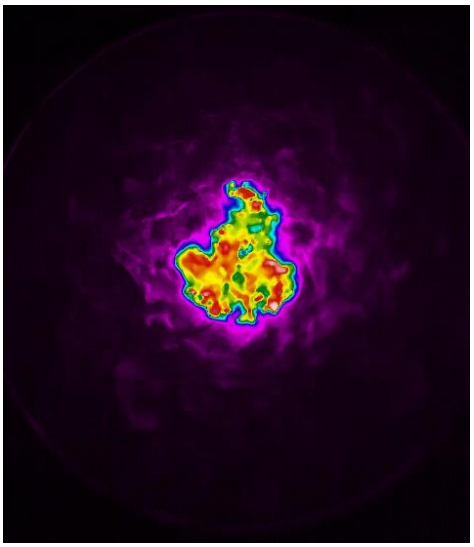

Fig. 7 Fire front movement at the beginning of fire test 2 (time 20 s)

The fire front reached the Eastern edge of the test dish in 73 s and the Northern edge in up to 146 s, while on the surface of the test dish there was also an area of unburned fuel (Figure 8).

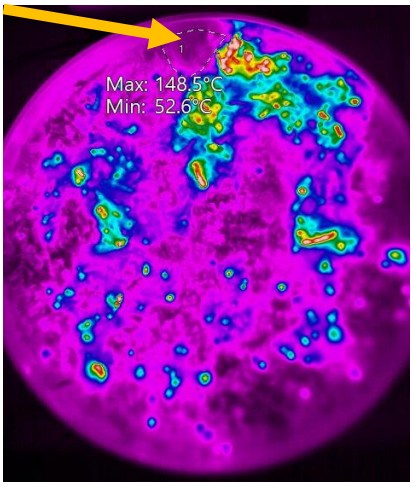

Fig. 8 Position of unburned area in fire test 2

3.1.2 Temperature course – data from the thermal imaging camera

The temperature course on the surface of the test sample was recorded for the position of the individual thermocouples, the entire test dish and subsequently on the individual profile lines. To determine the temperature of the surface of the test sample, recordings from a Fluke RSE600 thermal imaging camera were used, which were processed in the SmartView R&D software. Therefore, the temperatures were determined only within the framework of 2 fire tests carried out in the fume hood.

The thermal imaging camera records individual images at an interval of 0.1 s. In Fig. 9 and 10, we present the values in this interval, therefore we express the time units in the format h:min:s, not in seconds (s).

First, we present the results of the temperature course measured on the surface of the test sample detected at the positions of thermocouples T1-T5.

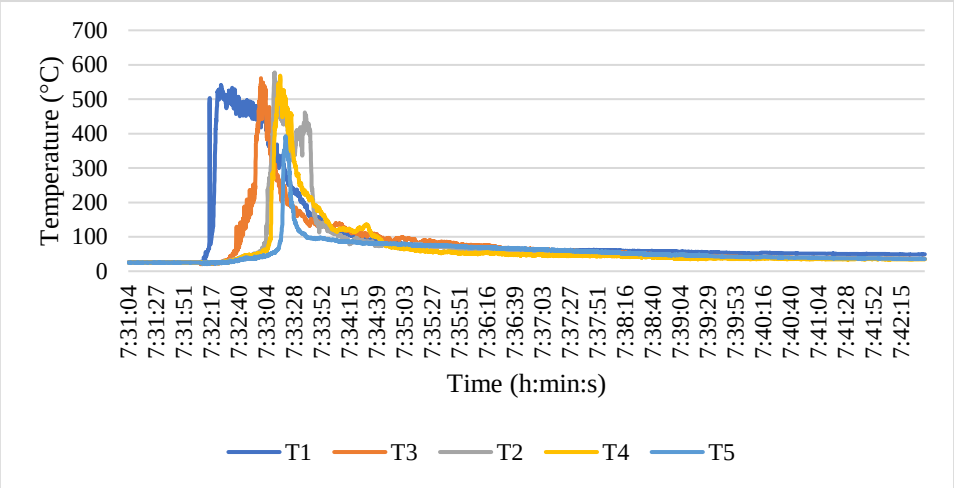

Fig. 9 Temperature course during fire test 1 recorded by thermocouples T1-T5

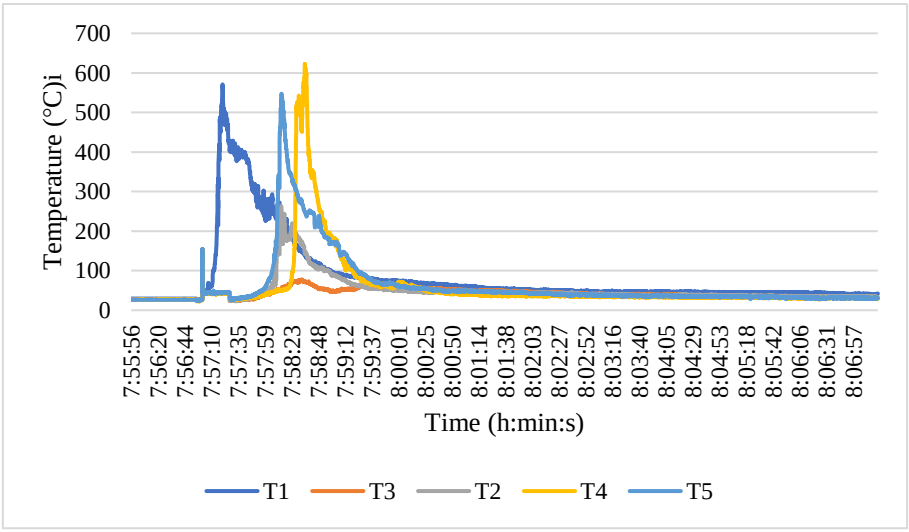

Fig. 10 Temperature course during fire test 2 recorded by thermocouples T1-T5

During the fire test, the maximum and average temperatures reached during the burning of beech litter were recorded on individual thermocouples. In Tab. 3 we provide an overview of these data, which are supplemented with the time in which this value was reached. At the same time, we also present outputs from the SmartView R&D program, i.e., images from the thermal imaging camera, capturing the surface of the test dish and the course of the temperature of the sample during the fire at the pre-defined times, calculated from the start of the fire test.

Tab. 3 Maximum and average temperatures recorded by thermocouples during the fire test carried out in the fume hood

Fire test	1		2	
/Thermocouple	T MAX (°C)	Time (s)	T MAX (°C)	Time
T1 (C)	541.7	13	571.0	7
T2 (W)	578.0	59	264.2	58
T3 (N)	560.9	48	78.4	80
T4 (E)	568.6	64	622.5	82
T5 (S)	392.3	69	547.4	61

Next, we present thermal images recorded at time of 13 s (Figure 11), 48 s (Figure 12), 59 s (Figure 13), 64 s (Figure 14) and 69 s (Figure 15) from the start of the fire test. These show the propagation of the fire during the fire test 1.

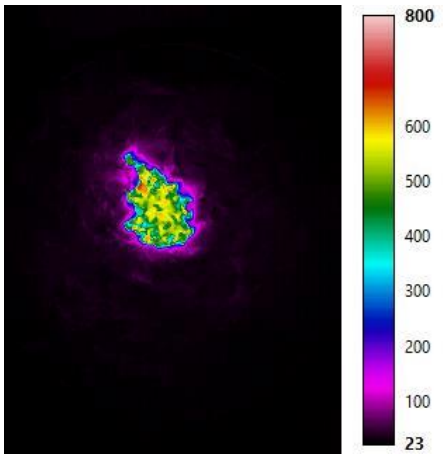

Fig. 11 Fire propagation during the fire test 1 – time of 13 s

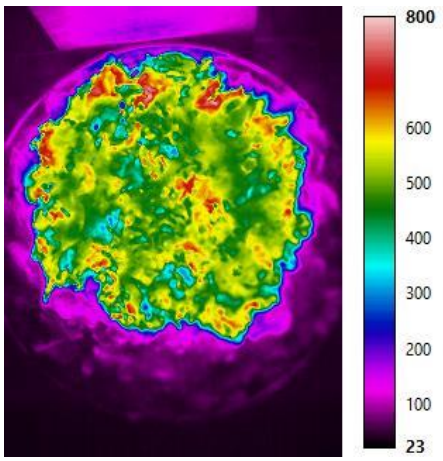

Fig. 12 Fire propagation during the fire test 1 – time of 48 s

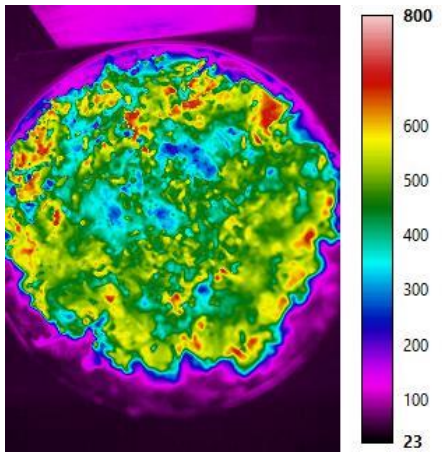

Fig. 13 Fire propagation during the fire test 1 – time of 59 s

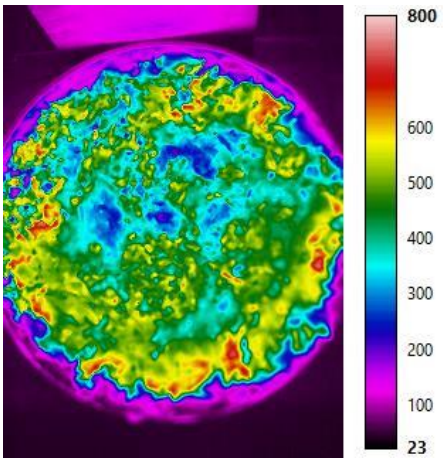

Fig. 14 Fire propagation during the fire test 1 – time of 64 s

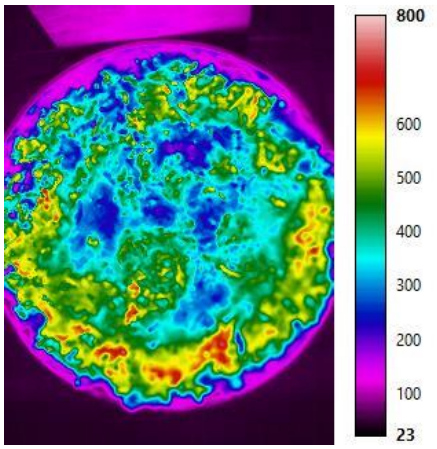

Fig. 15 Fire propagation during the fire test 1 – time of 69 s

The course of temperatures during fire test 1 calculated for the area of the entire test dish is presented in Figure 16.

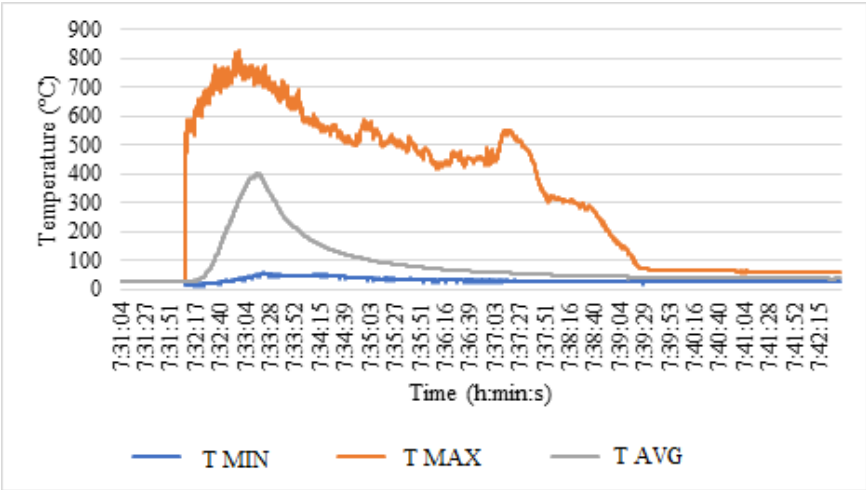

Fig. 16 Temperature course within the area of the test dish during fire test 1

During the fire test 1, the maximum temperature value of 770.6 °C was recorded at 21 s from the start of the fire test. At this time, the highest average temperature during the test was also recorded, namely 179.7 °C. At the time of the end of the test, there were no more spots on the surface of the test dish leading to re-ignition of the fire in case of a sudden supply of air.

The temperature during burning was automatically detected on profiles (4 profiles - eight cardinal points) created in the SmartView R&D software based on temperature information stored in infrared images acquired by the FLUKE thermal imaging camera.

3.1.3 Comparison of temperature course inside and on the surface of the fuel sample

The comparison of the temperature course on the surface and inside the fuel during the fire test was possible when providing the fire tests in the laboratory fume hood, together with using the FLUKE RSE600 thermal imaging camera.

We consider it necessary to draw attention to the fact that the performed study present ways of using progressive recording techniques and digital image analysis of images to derive important fire parameters that serve to understand fire dynamics. The objective of the study was not the analysis of the behaviour of forest litter during a fire itself. This would require the implementation of a sufficient number of fire tests, e.g., for the purpose of deriving dependencies between parameters. The results presented here also correspond to this fact.

Figures 17-22 show the results of the fire test 1 and data recorded by the thermocouples T1-T5.

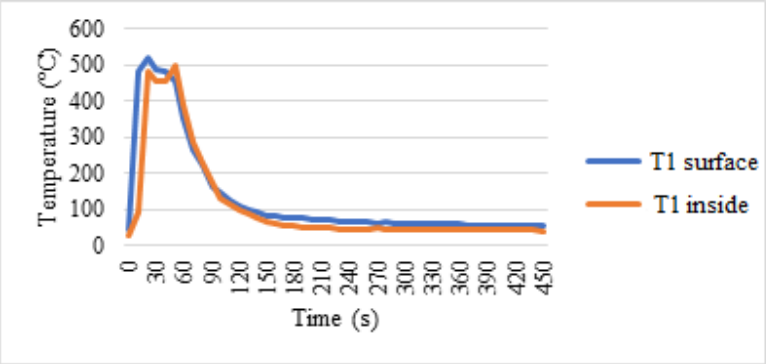

Fig. 17 Temperatures course comparison on the surface and inside the fuel - fire test 1 (hood), T2

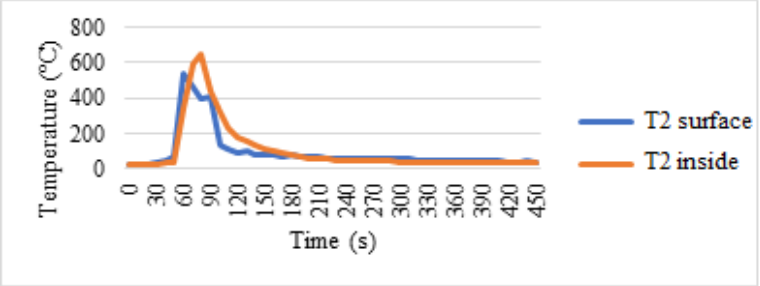

Fig. 18 Temperatures course comparison on the surface and inside the fuel - fire test 1 (hood), T2

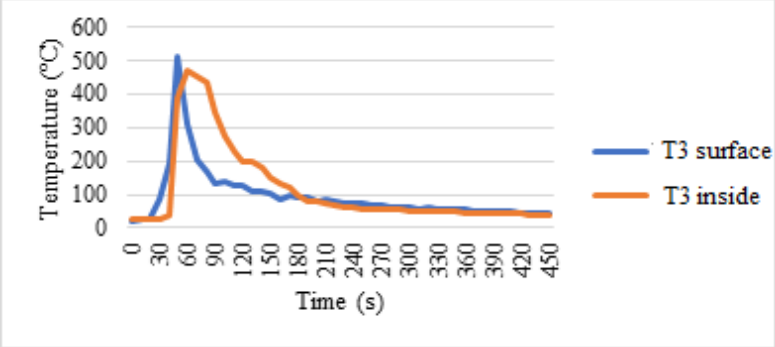

Fig. 19 Temperatures course comparison on the surface and inside the fuel – fire test 1 (hood), T3

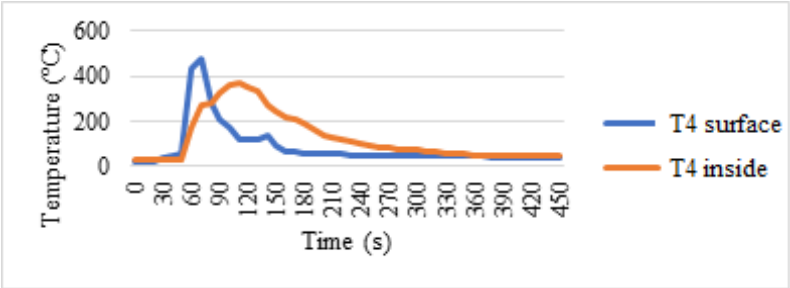

Fig. 20 Temperatures course comparison on the surface and inside the fuel – fire test 1 (hood), T4

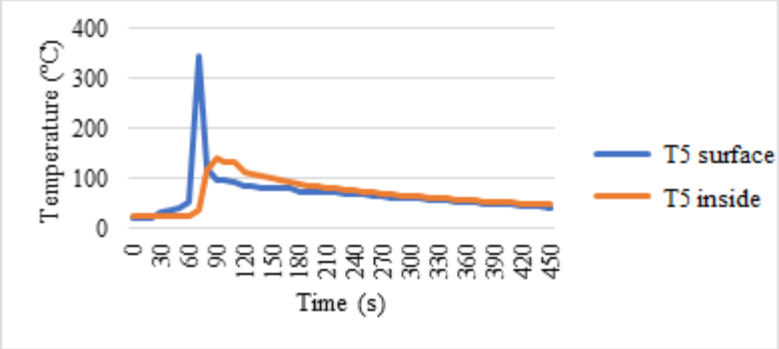

Fig. 21 Temperatures course comparison on the surface and inside the fuel – fire test 1 (hood), T5

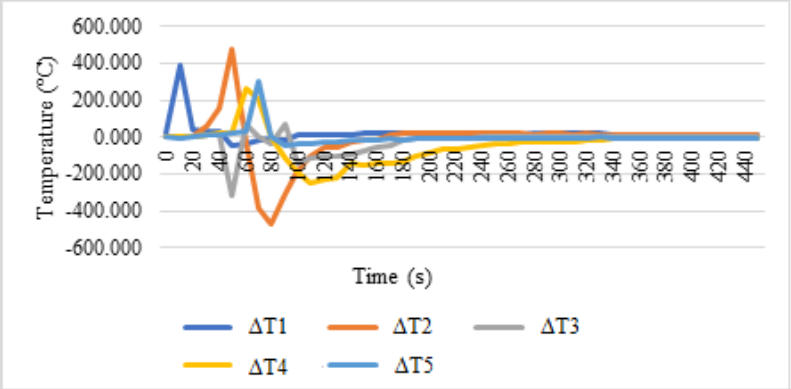

Fig. 22 Temperatures course comparison on the surface and inside the fuel – fire test 1 (hood), T1-T5

As seen from Fig. 22, the significant differences between the temperatures recorded by the thermocouples and the temperatures recorded by the thermal imaging camera were in the flame burning phase. The minimum (T MIN), maximum (T MAX) and average (T AVG) values of temperature differences at the position of individual thermocouples during fire tests are provided by Tab. 4.

Tab. 4 Values of temperature differences at the position of individual thermocouples during the fire test 1

Fire test /Thermocouple	1			2		
	Δ T MAX (°C)	Δ T MIN (°C)	Δ T AVG (°C)	Δ T MAX (°C)	Δ T MIN (°C)	Δ T AVG (°C)
T1 (C)	389.7	-45.0	24.7	452.7	-184.2	19.9
T2 (W)	473.8	-473.1	-11.3	157.0	-67.1	-2.4
T3 (N)	72.1	-319.7	-22.6	34.8	-316.4	-29.7
T4 (E)	258.4	-250.0	-42.2	437.9	-8.9	20.6
T5 (S)	305.3	-43.7	1.7	402.8	-8.4	27.1

3.2 Duration of flame burning and glowing/smouldering

The study of combustion during fire tests was divided into flame and flameless combustion phases. From the measured values and calculations, we determined 3 phases of combustion. While the flame burning phase itself took place in two sub-phases, i.e., phases of fire development and steady burning. Flameless combustion took place in the last phase called decay. While the highest mass loss, relative burning rate, highest temperatures and flame height were observed right during the flame burning. The rate of the flame burning allowed the fire to spread around the entire perimeter of the test dish. During flameless combustion, the values were stabilized and without significant changes until the end of the experiment. The transition from flameless combustion to flameless combustion was accompanied by smoke, which could be observed visually.

The duration of flame burning was detected from video images analysis. In Tab. 5 and 6, we present data on the duration of flame and flameless (smouldering/incandescence) burning (also as a percentage of the entire duration of the fire test, i.e., 600 s) for fire tests carried out in the laboratory chamber and for fire tests carried out in the laboratory fume hood. The burning was initiated by the flame of a match.

Tab. 5 Flame burning duration

Fire test	Flame burning duration (s)	Flame burning duration (%)
Chamber1	132	22
Chamber2	169	28
Chamber3	154	26
Hood1	176	29
Hood2	217	36
Average Chamber	152	25
Average Hood	166	28

Tab. 6 Glowing/smouldering duration

Fire test	Glowing/smouldering duration (s)	Glowing/smouldering duration (%)
Chamber1	328	55
Chamber2	271	45
Chamber3	296	49
Hood1	265	44
Hood2	min. 383	min. 64
Average Chamber	298	50

As seen from the results shown in Tab. 5 and Tab. 6, there are obvious differences in fire behaviour between the individual tests. The reason for this is mainly the fact that forest litter is not a homogeneous material in its structure, like e. g. wood. The behaviour of the fire in this case is mostly influenced by its distribution on the surface and the overall structure of the fuel. Even with the greatest effort to create test samples that will be similar. This will create a problem because such samples cannot be prepared with this type of material. However, this does not mean that it is not necessary to investigate them, on the contrary, we need to create an extensive set of data based on several fire tests and then try to derive dependencies between the parameters affecting the behaviour (dynamics) of the fire.

3.3 Flame height

In terms of flame height, several parameters were monitored. The maximum, mean and average flame height values were derived from the video data extracted for 5 s intervals of flame burning. Results are presented in Tab. 7 and Tab. 8.

Tab. 7 Average and maximum flame height

Fire test	Average flame height (m)	Maximum flame height (m)
Chamber1	0.24	0.52
Chamber2	0.20	0.72
Chamber3	0.16	0.50
Hood1	0.16	0.45
Hood2	0.08	0.21

Further, there are introduced results for mean flame height (Tab. 8).

Tab. 8 Mean height of the flame according to equation (3)

Fire test	Mean height of the flame (m)	Time (s)
Chamber1	0.16	65
Chamber2	0.02	85
Chamber3	0.04	80
Hood1	0.01	90
Hood2	0.03	110

Using the results of fire tests carried out in the fume hood, we created an algorithm that enables the automated calculation of the density of the radiated heat flux (equation 4) for the entire area of the test dish.

Here we only present the results for the maximum temperature values recorded in both fire tests.

In the case of fire test 1, the highest temperature, 770.6 °C, was recorded by the thermal imaging camera at time of 21 s from the start of the fire test. After substituting this temperature into equation (8), we obtained the value of the wavelength of the maximum radiation intensity at the level of 0.0038 mm = 3.8 μm (mid-wave infrared radiation – MWIR).

A higher maximum temperature value was reached during the fire test 2 (797.6 °C), within 65 s from the start of the test. In this case, the wavelength value of the maximum radiation intensity was calculated to be 0.0036 mm = 3.6 μm (MWIR).

Next, we present the result of the automated determination of the wavelength of the maximum radiation intensity in the form of a time profile of the density of the radiated heat flux calculated for the centre of the test dish (position T1).

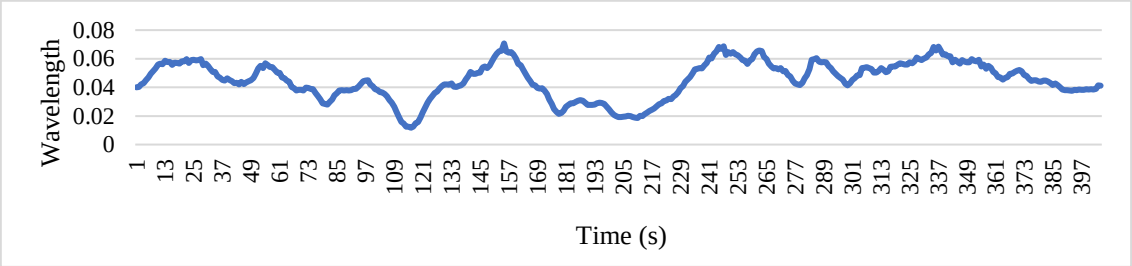

Fig. 23 Density of radiated heat flux in time in the centre of the dish (position T1)

These values are extracted from the generated image, where each pixel contains a wavelength value calculated according to formula (4). After converting the values from mm to μm and classifying (reclassifying) the wavelength values into the appropriate category, we obtain information about the type of infrared radiation and its spatial distribution on the surface of the sample (material).

3.4. Burning rate

From the point of view of calculating the burning rate, we focused on determining the relative mass burning rate and surface burning rate of fuel recorded on surface of the test dish.

3.4.1 Relative mass burning rate

We have expressed the mass burning rate based on the mass loss data, which was recorded during the tests with accurate scales from the RADWAG company. The fire test lasted a total of 600 s = 10 min.

In Figure 24 we present the results of mass loss for fire tests carried out in a laboratory chamber.

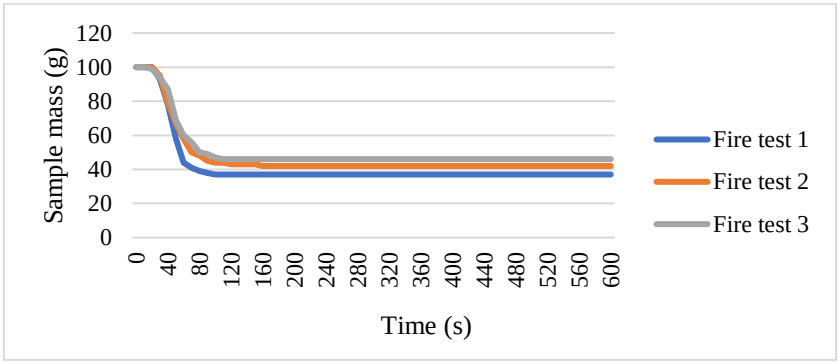

Fig. 24 Mass loss of samples during fire tests carried out in the chamber

Fig. 25 gives a view of the relative mass rate of burning of the samples during the implementation of fire tests in the laboratory chamber. We calculated this according to formula (2).

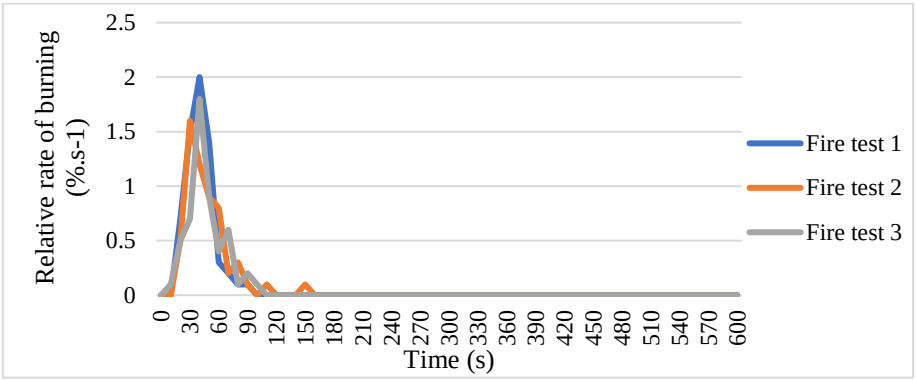

Fig. 25 Relative mass burning rate of samples during fire tests in the chamber

In Fig. 26, we introduce the results according to the mass loss of samples during fire tests provided in laboratory fume hood.

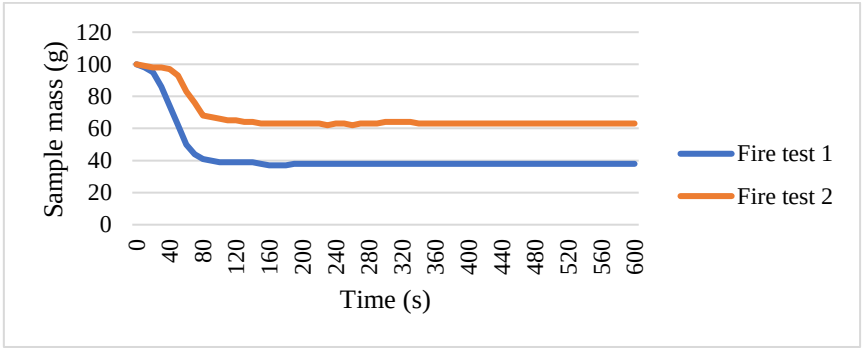

Fig. 26 Mass loss of samples during fire tests carried out in the fume hood

Fig. 27 provides an overview of the relative mass rate of burning of samples during fire tests in a laboratory fume hood.

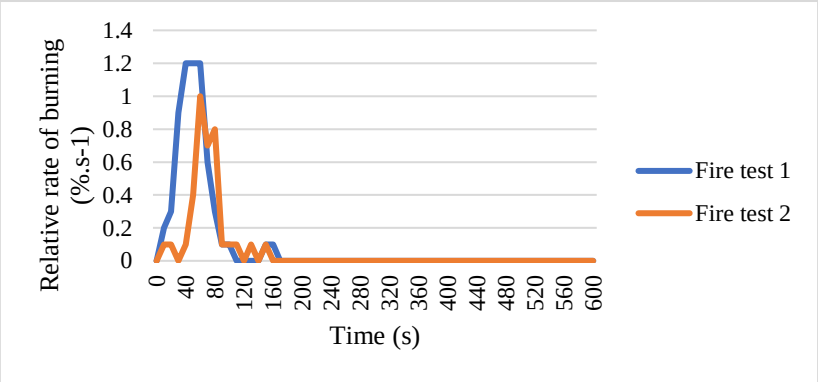

Fig. 27 Relative mass burning rate of samples during fire tests in the fume hood

3.4.2 Surface burning rate

The calculation of the surface burning rate was preceded by analyses aimed at determining the increase in the burning area (burning area with a temperature above 400 °C) within the test dish over time (time interval of 1 s). Here we present the results for fire test 1 (Fig. 28). At the same time, we also present the result regarding the extent of the fire area on which the temperature above 400°C was reached during the fire (Fig. 29).

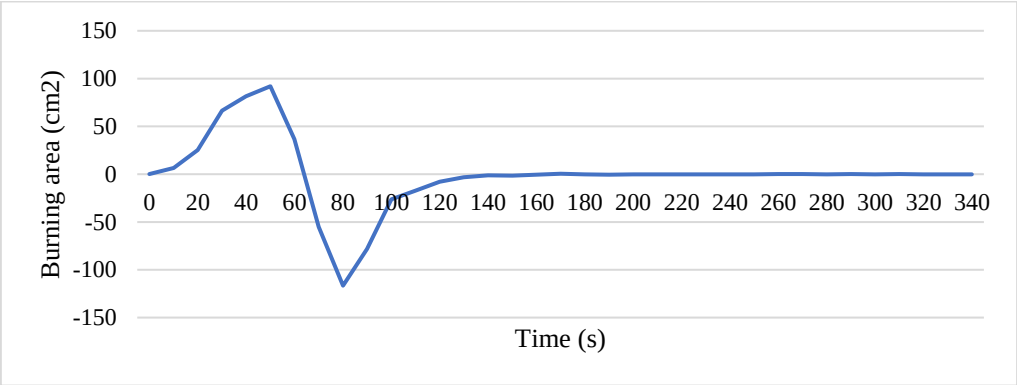

Fig. 28 Fire test 1 – Increase in burning area over time

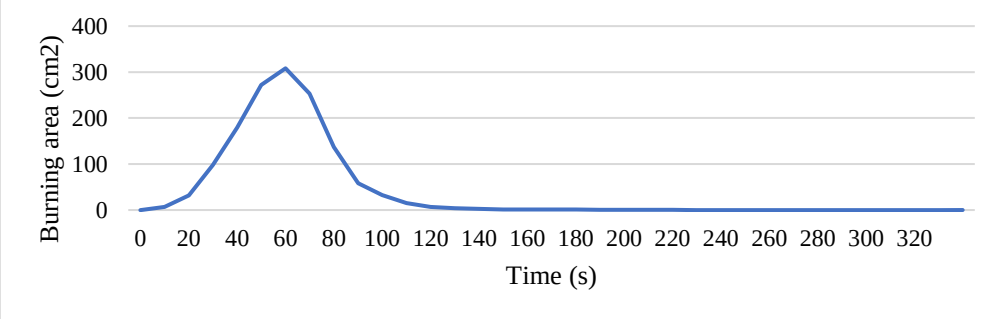

Fig. 29 Fire test 1 – Total burned area over time

From Fig. 27 and 28, it is obvious that the highest increase in the burning area is precisely in the phase of flame (steady) burning. While the maximum increase in the burning area was recorded in 50 s after the start of the fire test and represented a value of 92 cm^2. In the time 60 s after the start of the test, the largest burning area was reached, namely 308 cm^2.

The surface burning rate was calculated based on the algorithm developed in the Python programming language. In this subsection, we present the results of the image analysis for fire test 1, the images of which were also used for the development of an algorithm for the automated calculation of the area burning rate of the sample in 600 s.

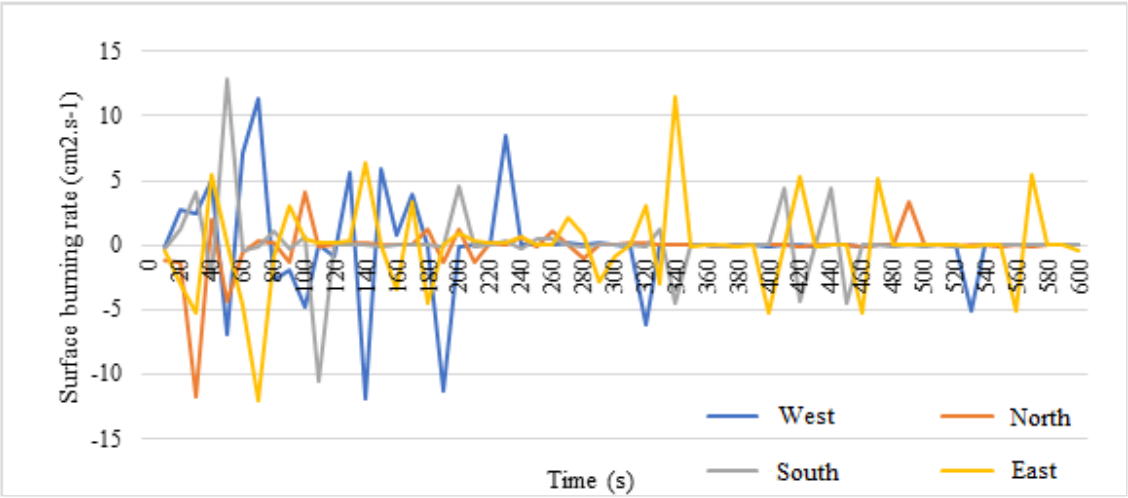

Fig. 30 Course of the surface burning rate in four directions in 10 s intervals

In Fig. 30, it is possible to detect phases in which the burning took place faster (flame burning phase) and phases where the burning rate values reached lower values (smouldering phase). In the direction to the south (to T5) from the centre of the bowl, the maximum value of the surface burning rate of 12.8 $cm^2 \cdot s^{-1}$ was reached in 50 s from the start of the fire test. In the direction to the west (to T2) from the centre of the bowl, the maximum value of the surface burning rate of 11.3 $cm^2 \cdot s^{-1}$ was reached in 70 s from the start of the fire test. In the direction to the east (to T4) from the centre of the bowl, the maximum value of the surface burning rate of 11.5 $cm^2 \cdot s^{-1}$ was reached in 340 s from the start of the fire test. In the direction to the north (to T3) from the centre of the bowl, the maximum value of the surface burning rate of 4.1 $cm^2 \cdot s^{-1}$ was reached in 100 s from the start of the fire test.

The values of the surface burning rate reached not only positive but also negative values. The reason is mainly fuel heterogeneity. In the case of a homogeneous fuel, the propagation would be constant, but the heterogeneity of the fuel caused differences in the time required for preheating the fuel and its subsequent ignition. At the same time, after burning off the fuel in the parts near the place of initiation, it subsequently cooled down, which caused the reduction of the total area with a temperature above 400°C.

In Fig. 31, we present the course of surface burning rate in 1 s intervals.

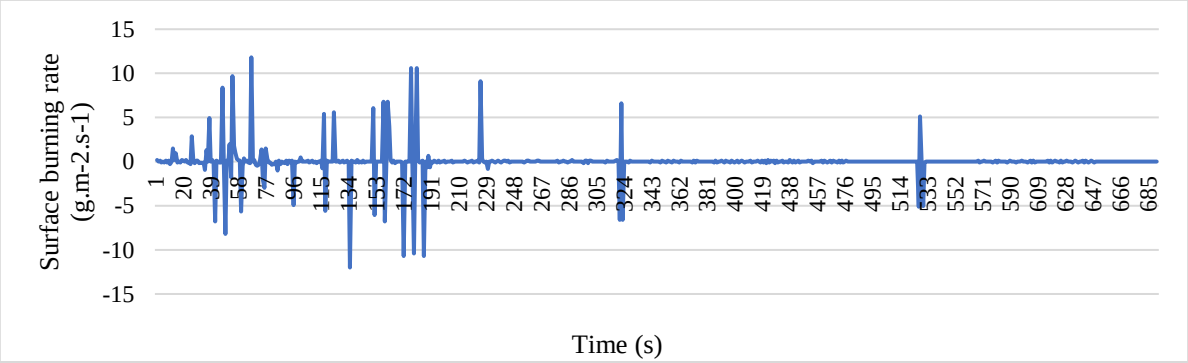

Fig. 31 Course of the surface burning rate in 1 s intervals

3.5 Automated delineation of flame outlines

For the completeness, we also present the image processing methodology/algorithm applicable in the Idrisi Terrset environment, as well as an example sample of the outputs from the image analyses aimed at identifying the flame outlines (2D visualization of the flame) from the sequence of frames obtained from the video recordings.

File/Import/Desktop Publishing Formats/JPGIDRIS (Output Reference Information/Plane)

File/Display/SEPARATE	Creates separated images (raster) from 24-bit colour or any other binary image in RGB channels. For further analyses select raster *Band 2.*
Digitize/Polygon	Serves for creation of polygon vector layer (test dish outline) based on raster file (image). Specify the name of the file and digitize the outline of the test dish by continual clicking on the left mouse button.
RASTERVECTOR	Converts the vector file with test dish outline to raster file. The spatial parameters of creating raster file should be copied from raster *Band 2* (select it from the list).
Idrisi GIS Analysis/Image Calculator	(*Raster file with outline of the test dish*raster Band2)* Creation of a raster reducing the image extent to area with test dish and flame.
Idrisi GIS Analysis/Database Query/Reclass	Reclassification of raster values into two classes based on thresholding the flame spectral values. (In study, the reclassification of raster values with threshold of 190 was applied for flame detection).
Composer/Add Layer/Vector	Visualization of the 2D surface of the flame within the test dish. Using this procedure, we overlay the raster image of the 2D flame with a vector one representing the outline of the dish (Fig. 32).

Fig. 32 Flame area during the fire test 1 in time of 20 s

Outputs (raster files) of image analysis from the Idrisi TerrSet environment can be further processed (calculation of flame height) in this environment these outputs can be used after exporting them to ASCII text format as input data to other program environments such as MATLAB to process further calculations.

4 Conclusions

The main objective of the study was to identify and verify the suitability of the applications of digital image analysis tools in fire engineering. For the processing of the study, the Fluke RSE600 thermal imaging camera was selected and procured after conducting market research regarding the available devices and their technical parameters. The Fluke RSE600 thermal imaging camera, including the supplied software, demonstrated not only the quality and accuracy of measurements, but also its

durability and ability to work in extreme conditions. The possibility of connecting via WIFI multiplies its usability in direct deployment.

We used several computer programs, libraries, and online tools to process and evaluate the measured data. We used several in duplicate to compare their usability for image analysis.

The results of the study are original. For the analyses, several progressive technologies were used, such as thermal imaging, digital technologies intended for the creation of video recordings, but also for pre-processing and image analysis of digital recordings, including infrared images.

As the benefit for the field of science, the study verified the possibilities and appropriateness of the application in the work of applied digital technologies for the study of fire behaviour and the automated derivation of its selected parameters (e.g., the development of temperatures during a fire over time on the surface of the sample, calculation of the area rate of burning over time, detection shape and height of the flame, etc.).

The study provides guidance for conducting similar experiments with the use of digital technologies aimed at studying fire behaviour, even in the case of other types of materials, as well as studying the dynamics of fires in closed spaces.

The implementation of thermal imaging camera and a video (optical) camera into the fire tests is a progressive method allowing further and deeper study of fire dynamics parameters which cannot be captured by human eye or measured another way. The digital outputs themselves are a key input to image analyses and the creation of algorithms enabling the automated derivation of selected fire parameters from them. And finally, use of thermal imaging helps researchers to understand the relationship of fuels and fire effects.

From the point of view of the fire test results achieved and presented here, it is necessary to state that due to the variability of conditions that significantly affect the behaviour of forest litter during a fire, it is necessary to carry out enough repetitions under the same conditions (environment, fuel moisture content, etc.), until the variability of the results will not be reduced to an acceptable level. However, this presupposes the initiation of extensive and long-term laboratory research.

Acknowledgments

This research was funded by the Slovak Research and Development Agency, grant number APVV-17-0005 (40 %) and grant number APVV-19-0612 (40 %); and by the European Commission, H2020-LC-GD-2020-3, project ID: 101037247 (20 %).

References

[1] Thomas P. 1963. The size of flames from natural fire. Proc. Combust. Inst. 9(1):844-859.

[2] Steward F. 1970. Prediction of the Height of Turbulent Diffusion Buoyant Flames. Combust. Sci. Technol. 2(4):203-212.

[3] Byram GM. 1957. Some principles of combustion and their significance in forest fires. Fire Manag. Today 18(2):47-57.

[4] Gill AM, Allan G. 2008. Large fires, fire effects and the fire-regime concept. Int. J. Wildland Fire 17(6):688-695.

[5] Arnold RK, Buck CC. 1954. Blow-up fires – silviculture or weather problems? J. For. 52(6):408-411.

[6] Pitts WM. 1991. Wind Effect on Fires. Prog. Energy Combust. Sci. 17(2):83-134.

[7] Stocks BJ, Mason JA, Todd JB et al. 2002. Large forest fires in Canada, 1959–1997. J. Geophys. Res. 108(D1):FFR 5-1-FFR 5-12.

[8] Koo E, Pagni PJ, Weise DR, Woycheese JP. 2010. Firebrands and spotting ignition in large-scale fires. Int. J. Wildland Fire 19(7):818-843.

[9] Countryman CM. 1964. Mass Fires and Fire Behavior. USDA Forest Service: Pacific Southwest Forest and Range Experiment Station, RS-RP-19.

[10] Countryman CM. 1965. Mass fire characteristics in large-scale tests. Fire Technol. 1(4):303-317.

[11] Baldwin R. 1966. Some Tentative Calculations of Flame Merging in Mass Fires. Joint Fire Research Organization, Fire Research Note 629.

[12] Byram GM. 1966. Scaling laws for modelling mass fires. Pyrodynamics 4(3):271-284.

[13] Countryman CM. 1969. PROJECT FLAMBEAU - An Investigation of Mass Fires (1964-1967). Pacific Southwest Forest and Range Experiment Station, Final Report - Volume I.

[14] Heskestad G. 1991. A reduced-scale mass fire experiment. Combust. Flame 83(3-4): 293-301.

[15] Finney Ma, McAllister SS. 2011. A review of fire interactions and mass fires. *J. Combust.* 2011:1-14.

[16] Viegas DX. 2012. Extreme fire behaviour. In Cruz, A.C.B., Correa, R.E.G. (Eds.). Forest Management: Technology, Practices and Impact. New York: Nova Science Publishers, pp. 1-56.

[17] Kalman, RE. 1960. A new approach to linear filtering and prediction problems. Transactions of the ASME–Journal of Basic Engineering 82:35–45.

[18] Britton CM, Karr BL, Sneva FA. 1977. A technique for measuring rate of spread. Journal of Range Management 30:395–397.

[19] Clements HB. 1983. Measuring fire behaviour with photography. Photogrammetric Engineering and Remote Sensing 49:213–217.

[20] Adkins CW. 1995. 'Users' guide for fire image analysis system – Version 5.0: a tool for measuring fire behavior characteristics.' USDA Forest Service, Southern Research Station, General Technical Report SE-93. (Asheville, NC)

[21] Clark TL, Radke L, Coen J, Middleton D. 1999. Analysis of small-scale convective dynamics in a crown fire using infrared video camera imagery. Journal of Applied Meteorology 38**:**1401–1420.

[22] Viegas DX, Cruz MG, Ribeiro LM, Silva AJ, Ollero A. et al. 2002. Gestosa fire spread experiments. In 'Proceedings of IV International Conference on Forest Fire Research and 2002 Wildland and Fire Safety Summit'. (Ed. DX Viegas) (CD-ROM) (Millpress: Rotterdam)

[23] Den Breejen E, Roos M, Schutte K, De Vries JS, Winkel H. 1998. Infrared Measurements of Energy Release and Flame Temperatures of Forest Fires. In 'Proceedings of the 3rd International Conference on Forest Fire Research'. November 1998, Luso, Portugal. (Ed. DX Viegas) pp. 517–532. (ADAU, University of Coimbra: Portugal)

[24] Martínez-De Dios JR, André JCS, Gonçalves JC, Arrue BCH, Ollero A, Viegas DX. 2006 Laboratory fire spread analysis using visual and infrared images. International Journal of Wildland Fire 15:179-186. https://doi.org/10.1071/WF05004.